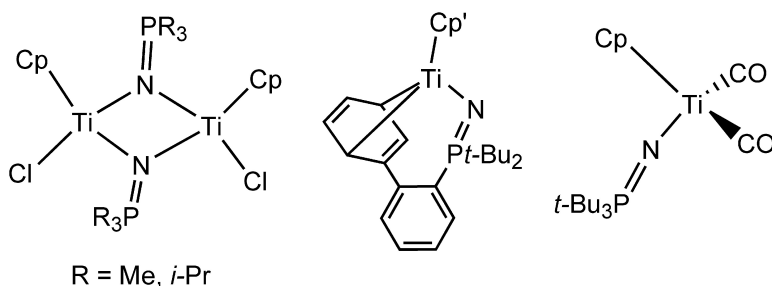


Reduction of Titanium(IV)-Phosphinimide Complexes: Routes to Ti(III) Dimers, Ti(IV)-Metallacycles, and Ti(II) Species

Todd W. Graham, James Kickham, Silke Courtenay, Pingrong Wei, and Douglas W. Stephan

Organometallics, 2004, 23 (13), 3309-3318 • DOI: 10.1021/om049826q

Downloaded from <http://pubs.acs.org> on December 12, 2008



More About This Article

Additional resources and features associated with this article are available within the HTML version:

- Supporting Information
- Links to the 4 articles that cite this article, as of the time of this article download
- Access to high resolution figures
- Links to articles and content related to this article
- Copyright permission to reproduce figures and/or text from this article

[View the Full Text HTML](#)



ACS Publications
High quality. High impact.

Reduction of Titanium(IV)-Phosphinimide Complexes: Routes to Ti(III) Dimers, Ti(IV)-Metallacycles, and Ti(II) Species

Todd W. Graham, James Kickham, Silke Courtenay, Pingrong Wei, and Douglas W. Stephan*

Chemistry and Biochemistry, University of Windsor, Windsor, Ontario, Canada, N9B 3P4

Received March 10, 2004

The redox chemistry of phosphinimide-containing group IV metal complexes has been investigated. Reaction of the simple phosphinimide species $\text{CpTi}(\text{NPR}_3)\text{Cl}_2$ ($\text{R} = \text{Me}$ **1**, *i*-Pr **2**) with Mg affords complexes formulated as $[\text{CpTiCl}(\mu\text{-NPR}_3)]_2$ ($\text{R} = \text{Me}$ **3**, *i*-Pr **4**). In contrast, $\text{CpTi}(\text{NP}t\text{-Bu}_3)\text{Cl}_2$ (**5**) is reduced by Mg to a putative Ti(II) species that can be intercepted by a variety of reagents including 2,3-dimethyl-1,3-butadiene, diphenylacetylene, phenylacetylene, bis(trimethylsilyl)acetylene, ethylene, and propylene to give monometallic metallacyclic complexes. In this fashion, the Ti(IV) metallacycles $\text{CpTi}(\text{NP}t\text{-Bu}_3)(\text{CH}_2\text{C}(\text{Me})\text{-C}(\text{Me})\text{CH}_2)$, **6**, $\text{CpTi}(\text{NP}t\text{-Bu}_3)(\text{CPh})_4$, **7**, $\text{CpTi}(\text{NP}t\text{-Bu}_3)(\text{C}(\text{Ph})\text{CHC}(\text{Ph})\text{CH})$, **8**, $\text{CpTi}(\text{NP}t\text{-Bu}_3)(\eta^2\text{-C}_2(\text{SiMe}_3)_2)$, **9**, $\text{CpTi}(\text{NP}t\text{-Bu}_3)(\text{CH}_2)_4$, **10**, $\text{CpTi}(\text{NP}t\text{-Bu}_3)(\text{CH}_2\text{CHMe})_2$, **15**, and $\text{CpTi}(\text{NP}t\text{-Bu}_3)(\text{CH}_2)_2(\text{CPh})_2$, **16**, were prepared. Related intramolecular formation of metallacycle complexes was achieved upon reduction of $\text{Cp}^*\text{Ti}(t\text{-Bu}_2(2\text{-C}_6\text{H}_4\text{Ph})\text{PN})\text{Cl}_2$ ($\text{Cp}^* = \text{Cp}$ **18**, Cp^* **19**). The products $[\text{Cp}^*\text{Ti}(\text{NP}t\text{Bu}_2(2\text{-C}_6\text{H}_4\text{Ph}))]$ ($\text{Cp}^* = \text{Cp}$ **20**, Cp^* **21**) contained η^6 -interactions between Ti and the 2-phenyl substituent of the biphenyl unit. While Ti(II)-phosphinimide complexes have proven difficult to handle due to their reactivity, an unequivocal example of a Ti(II) species was obtained via reduction of $\text{Cp}^*\text{Ti}(\text{NP}t\text{-Bu}_3)\text{Cl}_2$ (**11**) with Mg in the presence of CO, affording the species $\text{Cp}^*\text{Ti}(\text{NP}t\text{-Bu}_3)(\text{CO})_2$ (**22**). X-ray data for **4**, **6**, **7**, **9**, **10**, **15**, and **17–22** are reported.

Introduction

Phosphinimide ligand complexes of transition metal and main group elements have been the subject of numerous studies and reviews.^{1,2} Recently our attention has focused on transition metal complexes containing sterically demanding phosphinimide ligands, as these systems mimic cyclopentadienyl groups, affording highly efficient olefin polymerization catalysts.^{3,4} Our studies have indicated that such ligands provide effective steric protection of the active site and at the same time offer increased accessibility of the metal center to substrate molecules.⁵ In less sterically demanding systems, the accessibility of the phosphinimide N donor atom prompts the formation of bridging phosphinimide units in di-, tri-, and tetrametallic aggregates.¹ We have previously shown that the interaction of the phosphinimide N atom in the less sterically demanding systems results in reaction with AlMe_3 , prompting multiple C–H bond

activations of Ti–Me units, affording unprecedented carbide derivatives.^{6–8} In an effort to further study the fundamental chemistry of Ti-phosphinimide complexes, we are exploring their reduction chemistry. We have previously reported that the reduction of $\text{CpTi}(\text{NP}t\text{-Bu}_3)\text{Cl}_2$ by Mg in benzene affords the dimer $[\text{CpTi}(\text{NP}t\text{-Bu}_3)(\mu\text{-Cl})]_2$. This chloro-bridged species was characterized in the solid state by both X-ray crystallography and single-crystal EPR spectroscopy.⁹ In this paper, we probe phosphinimide ligand effects on the redox chemistry of these species. In these cases, the products derived include Ti(III) dimers, Ti(IV) metallacycles, and the first formal Ti(II)-phosphinimide derivative. The implications of these results are discussed and the potential for the utility of such redox chemistry considered.

Experimental Section

General Data. The syntheses were performed employing an atmosphere of dry, oxygen-free nitrogen in a Vacuum Atmospheres inert atmosphere glovebox or standard Schlenk techniques. Solvents were purified employing Grubbs type column systems manufactured by Innovative Technology. ^1H , $^{13}\text{C}\{^1\text{H}\}$, and $^{31}\text{P}\{^1\text{H}\}$ NMR data were acquired on a Bruker

* Corresponding author. Fax: 519-973-7098. E-mail: Stephan@uwindsor.ca.

(1) Dehnicke, K.; Krieger, M.; Massa, W. *Coord. Chem. Rev.* **1999**, *182*, 19–65.

(2) Dehnicke, K.; Weller, F. *Coord. Chem. Rev.* **1997**, *158*, 103–169.

(3) Stephan, D. W.; Guerin, F.; Spence, R. E. v. H.; Koch, L.; Gao, X.; Brown, S. J.; Swabey, J. W.; Wang, Q.; Xu, W.; Zoricak, P.; Harrison, D. G. *Organometallics* **1999**, *18*, 2046–2048.

(4) Stephan, D. W.; Stewart, J. C.; Guerin, F.; Spence, R. E. v. H.; Xu, W.; Harrison, D. G. *Organometallics* **1999**, *18*, 1116–1118.

(5) Stephan, D. W.; Stewart, J. C.; Guerin, F.; Courtenay, S.; Kickham, J. E.; Hollink, E.; Beddie, C.; Hoskin, A. J.; Graham, T.; Wei, P.; Spence, R. E. v. H.; Xu, W.; Koch, L.; Gao, X.; Harrison, D. G. *Organometallics* **2003**, *22*, 1937–1947.

(6) Kickham, J. E.; Guerin, F.; Stewart, J. C.; Urbanska, E.; Ong, C. M.; Stephan, D. W. *Organometallics* **2001**, *20*, 3209.

(7) Kickham, J. E.; Guerin, F.; Stephan, D. W. *J. Am. Chem. Soc.* **2002**, *124*, 11486–11494.

(8) Kickham, J. E.; Guerin, F.; Stewart, J. C.; Stephan, D. W. *Angew. Chem., Int. Ed.* **2000**, *39*, 3263–3266.

(9) Sung, R. C. W.; Courtenay, S.; McGarvey, B. R.; Stephan, D. W. *Inorg. Chem.* **2000**, *39*, 2542–2546.

Avance 300 or 500 MHz spectrometer. ^1H and ^{13}C NMR chemical shifts are listed downfield from SiMe_4 in parts per million (ppm) and were referenced to the residual proton or carbon peak of the solvent. ^{31}P NMR data were referenced using an external standard relative to 85% H_3PO_4 . All NMR spectra were recorded in C_6D_6 unless otherwise stated. Galbraith Laboratories Inc. or in-house EA services performed the combustion analyses. In the case of compounds **9**, **14**, and **15** repeated attempts to obtain satisfactory carbon analyses, even with use of added oxidant, were unsuccessful. We have previously attributed such problems to partial formation of Ti-C during combustion of the Ti-organometallic derivatives.¹⁰ C_6D_6 and CD_2Cl_2 were purchased from Canadian Isotopes Laboratories; C_6D_6 and CD_2Cl_2 were vacuum distilled before use from Na/benzophenone and CaH_2 , respectively. $\text{CpTi}(\text{NPMe}_3)\text{Cl}_2$, **1**, $\text{CpTi}(\text{NP}i\text{-Pr}_3)\text{Cl}_2$, **2**, $\text{CpTi}(\text{NP}t\text{-Bu}_3)\text{Cl}_2$, **5**, $\text{Cp}^*\text{Ti}(\text{NP}t\text{-Bu}_3)\text{Cl}_2$, **11** and (indenyl) $\text{Ti}(\text{NP}t\text{-Bu}_3)\text{Cl}_2$, **13** were prepared as previously published.^{10,11} $\text{Pt-Bu}_2(2\text{-C}_6\text{H}_4\text{Ph})$ was purchased from the Strem Chemical Co.

Synthesis of $[\text{CpTiCl}(\mu\text{-NPR}_3)]_2$ ($\text{M} = \text{Me}$ **3, $i\text{-Pr}$ **4**).** These compounds were prepared in a similar manner, and thus one such preparation is detailed. A solution of **2** (430 mg, 1.117 mmol) in 5 mL of THF was added at -80°C to a suspension of Mg powder (100 mg, 4.114 mmol) in THF (5 mL). The mixture was warmed to 25°C and stirred for 1 h, over which time a brown solution was obtained. The solvent was removed in vacuo, and the residue was extracted with 5×5 mL of methylene chloride. The extracts were filtered through Celite, and then the solvent was removed. The brown solid was triturated with pentane and was then dried in vacuo. **3**: Yield: 65%. ^1H NMR: 5.88 (s, 5H, Cp); 0.87 (d, $^3J_{\text{HH}} = 13$ Hz, Me). $^{31}\text{P}\{^1\text{H}\}$ NMR: 36.7. Anal. Calcd for $\text{C}_{16}\text{H}_{28}\text{P}_2\text{N}_2\text{Ti}_2\text{Cl}_2$: C, 40.3; H, 5.2; N, 5.9. Found: C, 40.2; H, 5.1; N, 5.7. **4**: Yield: 54%. ^1H NMR: 6.17 (s, 5H, Cp); 2.15 (sept., $^3J_{\text{HH}} = 7$ Hz, 3H, CH); 1.03 (dd, $^3J_{\text{HH}} = 7$ Hz, $^3J_{\text{PH}} = 14$ Hz, 18H, Me). $^{31}\text{P}\{^1\text{H}\}$ NMR: 57.6. Anal. Calcd for $\text{C}_{28}\text{H}_{52}\text{P}_2\text{N}_2\text{Ti}_2\text{Cl}_2$: C, 52.1; H, 8.1; N, 4.3. Found: C, 51.9; H, 7.9; N, 4.2.

Synthesis of $\text{CpTi}(\text{NP}t\text{-Bu}_3)(\text{CH}_2\text{C}(\text{Me})\text{C}(\text{Me})\text{CH}_2)$, **6.** To a solution of **5** (200 mg, 0.50 mmol) in 10 mL of THF was added Mg powder (15 mg, 0.616 mmol). The solution was stirred for 5 min, then 2,3-dimethyl-1,3-butadiene (41 mg, 0.50 mmol) in 1 mL of THF was added. After stirring for 24 h, the solvent was removed in vacuo, and the resulting brown oily residue was taken up in 5 mL of toluene. After filtration through Celite the solvent was removed and the residue was washed several times with hexanes, affording a dark brown solid in 85% yield. $^{31}\text{P}\{^1\text{H}\}$ NMR (tol- d_6): 33.3. ^1H NMR (tol- d_6): 5.63 (s, 5H, Cp), 3.28 (d, $^2J_{\text{H-H}} = 7$ Hz, 2H, CH_2), 1.73 (s, 6H, Me), 1.50 (d, $^2J_{\text{H-H}} = 7$ Hz, 2H, CH_2), 1.17 (d, $^3J_{\text{P-H}} = 12$ Hz, 27H, $t\text{-Bu}$). $^{13}\text{C}\{^1\text{H}\}$ NMR (tol- d_6): 104.8, 62.1, 40.9 (d, $^1J_{\text{P-C}} = 46$ Hz), 30.0, 23.9. Anal. Calcd for $\text{C}_{23}\text{H}_{42}\text{NPTi}$: C, 67.1; H, 10.3; N, 3.4. Found: C, 66.8; H, 10.0; N, 3.2.

Synthesis of $\text{CpTi}(\text{NP}t\text{-Bu}_3)(\text{CPh})_4$, **7, $\text{CpTi}(\text{NP}t\text{-Bu}_3)(\text{C}(\text{Ph})\text{CHC}(\text{Ph})\text{CH})$, **8**, and $\text{CpTi}(\text{NP}t\text{-Bu}_3)(\eta^2\text{-C}_2(\text{SiMe}_3)_2)$, **9**.** These species were prepared in a similar manner, and only one representative procedure is provided. A 5 mL portion of THF was added to 100 mg (0.250 mmol) of $\text{CpTi}(\text{NP}t\text{-Bu}_3)\text{Cl}_2$ and 50 mg (2.057 mmol) of Mg powder, and the mixture was cooled to -35°C . Diphenylacetylene (90 mg, 0.501 mmol) was then added, and the mixture was stirred for 90 min. The solvent was removed in vacuo, and then the residue was extracted with 3×5 mL of ether (for **7**) or pentane (for **8** and **9**); the extracts were filtered through Celite and then the solvent was removed. **7**: Yield: 75%. $^{31}\text{P}\{^1\text{H}\}$ NMR: 37.0. ^1H NMR: 7.03 (m, 8H, Ph); 6.95 (m, 4H, Ph); 6.87 (m, 2H, Ph);

6.39 (s, 5H, Cp); 1.18 (d, $^3J_{\text{P-H}} = 13$ Hz, 27H, $t\text{-Bu}$). $^{13}\text{C}\{^1\text{H}\}$ NMR: 203.1, 148.7, 142, 131.4, 127.4, 127.1, 124.8, 123.0, 41.1 (d, $^1J_{\text{PC}} = 40.4$ Hz), 29.4. Anal. Calcd for $\text{C}_{45}\text{H}_{52}\text{NPTi}$: C, 78.8; H, 7.6; N, 2.0. Found: C, 78.6; H, 7.7; N, 1.7. **8**: Yield: 70%. $^{31}\text{P}\{^1\text{H}\}$ NMR: 35.9. ^1H NMR: 8.05 (d, $^4J_{\text{HH}} = 4$ Hz, $\text{CHC}(\text{Ph})\text{CH}$); 7.64 (m, 2H, Ph); 7.58 (d, $^4J_{\text{HH}} = 4$ Hz, 2H, TiCH); 7.30 (m, 6H, Ph); 7.12 (m, 2H, Ph); 6.30 (s, 5H, Cp), 1.18 (d, $^3J_{\text{PH}} = 15$ Hz, 27H, $t\text{-Bu}$). $^{13}\text{C}\{^1\text{H}\}$ NMR: 203.2, 149.3, 145.4, 142.1, 129.3, 128.8, 127.1, 126.4, 126.3, 125.4, 111.3, 41.7 (d, 45.7 Hz), 29.9. Anal. Calcd for $\text{C}_{33}\text{H}_{44}\text{NPTi}$: C, 74.3; H, 8.3; N, 2.6. Found: C, 73.1; H, 7.9; N 2.3. **9**: red-brown crystals. Yield: 80%. $^{31}\text{P}\{^1\text{H}\}$ NMR: 31.8. ^1H NMR: 6.70 (s, 5H, Cp); 1.56 (d, $^3J_{\text{PH}} = 13$ Hz, 27H, $t\text{-Bu}$); 0.08 (s, 18H, SiMe_3). $^{13}\text{C}\{^1\text{H}\}$ NMR (partial): 113.6, 41.7 (d, $^1J_{\text{PC}} = 47$ Hz); 30.4, 1.5. IR: ν_{CO} (KBr , cm^{-1}) 1597. Anal. Calcd for $\text{C}_{25}\text{H}_{50}\text{NPSi}_2\text{Ti}$: C, 60.1; H, 10.1; N, 2.8. Found: C, 59.1; H, 10.1; N, 2.8.

Synthesis of $\text{CpTi}(\text{NP}t\text{-Bu}_3)(\text{CH}_2)_4$, **10, $\text{Cp}^*\text{Ti}(\text{NP}t\text{-Bu}_3)(\text{CH}_2)_4$, **12**, (indenyl) $\text{Ti}(\text{NP}t\text{-Bu}_3)(\text{CH}_2)_4$, **14**, and $\text{CpTi}(\text{NP}t\text{-Bu}_3)(\text{CH}_2\text{CHMe})_2$, **15**.** These compounds were prepared in a similar manner, and thus one such preparation is detailed. A 10 mL portion of THF was added to **5** (227 mg, 0.567 mmol) and Mg powder (100 mg, 4.114 mmol) in a 400 mL heavy-walled glass vessel. The mixture was degassed by with two freeze-pump-thaw cycles and was then cooled to -80°C unless otherwise noted. Ethylene was admitted to the flask to a pressure of ca. 1 atm, after which the flask was sealed and the mixture warmed to room temperature. After stirring for 90 min, the solvent was removed in vacuo and the residue was extracted with 5×5 mL of pentane. The extracts were filtered through Celite, and the solvent was then removed in vacuo, yielding 153 mg (70%) of **10**. Yield: 80%. Crystalline material may be obtained by crystallization from ether at -35°C . $^{31}\text{P}\{^1\text{H}\}$ NMR: 32.8. ^1H NMR: 6.30 (s, 5H, Cp); 2.58 (m, 2H, TiCH_2CH_2); 2.18 (m, 2H, CH_2CH_2); 1.75 (t, $^3J_{\text{HH}} = 6$ Hz, 4H, CH_2CH_2); 1.26 (d, $^3J_{\text{PH}} = 13$ Hz, 27H, $t\text{-Bu}$). $^{13}\text{C}\{^1\text{H}\}$ NMR: 112.0, 55.8, 41.7 (d, $^1J_{\text{PC}} = 84$ Hz); 32.2, 30.2. Anal. Calcd for $\text{C}_{21}\text{H}_{40}\text{NPTi}$: C, 65.5; H, 10.5; N, 3.6. Found: C, 65.3; H, 10.5; N, 3.6. **12**: This reaction was done at -80°C . Yield: 85%. $^{31}\text{P}\{^1\text{H}\}$ NMR: 32.1. ^1H NMR: 2.49 (m, 2H, TiCH_2); 2.05 (s, 15H, Cp^*); 1.92 (m, 2H, TiCH_2); 1.38 (d, $^3J_{\text{PH}} = 8$ Hz, 27H, $t\text{-Bu}$); 1.25 (m, 2H, CH_2CH_2); 0.99 (m, 2H, CH_2CH_2). $^{13}\text{C}\{^1\text{H}\}$ NMR: 119.0, 59.8, 41.9 (d, $^1J_{\text{PC}} = 47$ Hz), 31.7, 30.6, 12.7. Anal. Calcd for $\text{C}_{26}\text{H}_{40}\text{NPTi}$: C, 70.1; H, 9.1; N, 3.1. Found: C, 67.6; H, 11.18; N, 3.0. **14**: Yield 60%. $^{31}\text{P}\{^1\text{H}\}$ NMR: 33.1. ^1H NMR: 7.75 (m, 2H, indenyl); 7.24 (m, 2H, indenyl); 6.29 (d, $^3J_{\text{HH}} = 3$ Hz, 2H, indenyl), 5.82 (t, $^3J_{\text{HH}} = 3$ Hz, 1H, indenyl); 2.34 (m, 4H, CH_2CH_2), 1.64 (m, 4H, CH_2CH_2); 1.26 (d, $^3J_{\text{PH}} = 13$ Hz, 27H, $t\text{-Bu}$). $^{13}\text{C}\{^1\text{H}\}$ NMR: 127.9, 125.8, 124.3, 114.6, 101.2, 61.7, 41.8, 32.3, 30.4. Anal. Calcd for $\text{C}_{27}\text{H}_{42}\text{NPTi}$: C, 69.0; H, 9.7; N, 3.2. Found: C, 66.8; H, 10.0; N, 3.2. **15**: Propene was added at -40°C , and the mixture was warmed to 25°C and stirred for 90 min. Yield: 96%. $^{31}\text{P}\{^1\text{H}\}$ NMR: 32.1. ^1H NMR: 6.27 (s, 5H, Cp); 2.58 (m, 1H, CH); 2.12, (dd, $^3J_{\text{HH}} = 11$ Hz, $^2J_{\text{HH}} = 11$ Hz, 1H, CH_2); 1.85 (dd, $^3J_{\text{HH}} = 12$ Hz, $^3J_{\text{HH}} = 12$ Hz, 1H, CH_2); 1.70 (m, 1H, CH); 1.33 (dd, $^2J_{\text{HH}} = 11$ Hz, $^3J_{\text{HH}} = 5$ Hz, 1H, CH_2); 1.26 (d, $^3J_{\text{PH}} = 13$ Hz, 27H, $t\text{-Bu}$); 1.10 (d, $^3J_{\text{HH}} = 6$ Hz, 3H, Me); 1.08 (d, $^3J_{\text{HH}} = 6$ Hz, 3H, Me); 1.04 (dd, $^2J_{\text{HH}} = 11$ Hz, $^3J_{\text{HH}} = 5$ Hz, 1H, CH_2). ^{13}C NMR: 112.0, 66.3, 66.1, 45.7, 44.5, 41.7 (d, $^1J_{\text{PC}} = 47$ Hz) 30.2, 26.4, 26.2. Anal. Calcd for $\text{C}_{23}\text{H}_{44}\text{NPTi}$: C, 66.8; H, 10.7; N, 3.4. Found: C, 62.9; H, 10.7; N, 3.7.

Synthesis of $\text{CpTi}(\text{NP}t\text{-Bu}_3)(\text{CH}_2)_2(\text{CPh})_2$, **16.** A 34 mg (0.191 mmol) sample of diphenylacetylene in 1.5 mL of benzene was added to 73 mg (0.189 mmol) of **10** in 1.5 mL of benzene. The mixture was stirred for 40 min, and then the solvent was removed in vacuo. Yield: 90%. $^{31}\text{P}\{^1\text{H}\}$ NMR: 34.7. ^1H NMR: 7.50 (m, 2H, Ph); 7.28–6.91 (m, 8H, Ph); 6.30 (s, 5H, Cp); 3.24 (m, 2H, TiCH_2CH_2); 2.20 (m, 1H, TiCH_2); 1.80 (m, 1H, TiCH_2); 1.24 (d, $^3J_{\text{PH}} = 12.9$ Hz, 27H, $t\text{-Bu}$). Anal. Calcd for $\text{C}_{33}\text{H}_{46}\text{NPTi}$: C, 74.0; H, 8.6; N, 2.6. Found: C, 73.8; H, 8.4; N, 2.5.

(10) Stephan, D. W.; Stewart, J. C.; Guérin, F.; Courtenay, S.; Kickham, J.; Hollink, E.; Beddie, C.; Hoskin, A.; Graham, T.; Wei, P.; Urbanska, E.; Spence, R. E. v. H.; Xu, W.; Koch, L.; X.Gao; Harrison, D. G. *Organometallics* **2003**, *22*, 1937–1947.

(11) Guérin, F.; Beddie, C. L.; Stephan, D. W.; Spence, R. E. v. H.; Wurz, R. *Organometallics* **2001**, *20*, 3466–3475.

Synthesis of *t*-Bu₂(2-C₆H₄Ph)PNSiMe₃, **17.** *t*-Bu₂(2-C₆H₄-Ph)P (2.055 g, 6.89 mmol) and azidotrimethylsilane (5.0 mL, 38 mmol) were combined in a 100 mL Schlenk flask. The slurry was refluxed vigorously for two weeks, during which time the phosphine dissolved and the solution developed a lemon-yellow color. Excess azidotrimethylsilane was removed in vacuo, and the solid was recrystallized from pentane. Yield: 1.319 g; 50%. ³¹P{¹H} NMR: 22.3. ¹H NMR: 7.54 (m, 1H, Ph); 7.20 (m, 5H, H_e); 6.90 (m, 3H, Ph); 1.15 (d, ³J_{PH} = 14 Hz, 18H, *t*-Bu). 0.07 (s, 9H, SiMe₃). ¹³C{¹H} NMR: 149.7, 144.2, 135.3 (d, ¹J_{PC} = 8 Hz), 131.0 (d, ²J_{PC} = 14 Hz), 129.7 (s, Ph), 129.2, 128.3, 127.7, 126.3, 124.6 (d, ⁴J_{PC} = 12 Hz), 38.4 (d, ¹J_{PC} = 57 Hz), 28.7, 4.6. Anal. Calcd for C₂₃H₃₆NPSi: C, 71.6; H, 9.4; N, 3.6. Found: C, 71.5; H, 9.2; N, 3.7.

Synthesis of Cp*Ti(NP*t*-Bu₂(2-C₆H₄Ph))Cl₂ (Cp' = Cp **18, Cp* **19**).** These compounds were prepared in a similar fashion, and thus one preparation is detailed. Compound **17** (1.006 g, 2.61 mmol) and CpTiCl₃ (0.514 g, 2.34 mmol) were added to a 400 mL glass bomb with 70 mL of toluene. The flask was evacuated, sealed, and heated at 75 °C for 48 h. The yellow solution was filtered through Celite, and the solvent was removed in vacuo. The yellow solid was washed with hexanes (3 × 10 mL) and dried under vacuum. Yield: 1.036 g; 89%. **18**: ³¹P{¹H} NMR: 45.5 (75%, major); 31.7 (25%, minor). ¹H NMR: 9.19 (dd, ³J_{HH} = 9 Hz, ³J_{PH} = 13 Hz, 1 H, Ph); 7.39 (br, 1 H, Ph); 7.30 (t, ³J_{HH} = 8 Hz, 1 H, Ph); 6.94 (m, 5 H, Ph); 6.80 (dd, ³J_{HH} = 5 Hz, ⁴J_{PH} = 5 Hz, 1 H, Ph); 6.48 (s, Cp, major); 6.11 (s, Cp, minor); 1.28 (d, ³J_{PH} = 15 Hz, *t*-Bu, minor); 1.00 (s, ³J_{PH} = 15 Hz, *t*-Bu, major). ¹³C{¹H} NMR: 144.2, 143.9, 139.3 (d, ²J_{CP} = 8 Hz), 133.4 (d, ⁴J_{CP} = 11 Hz), 131.0, 130.7, 128.3, 127.7, 127.2 (d, ³J_{CP} = 10 Hz), 116.2 (s, Cp, minor), 115.3 (s, Cp, major), 42.6 (d, ¹J_{CP} = 50 Hz, *t*-Bu, minor); 39.7 (d, ¹J_{CP} = 50 Hz, *t*-Bu, major), 28.8 (s, *t*-Bu, minor), 27.7 (s, *t*-Bu, major). Anal. Calcd for C₂₅H₃₂Cl₂NPTi: C, 65.5; H, 5.7; N, 12.5. Found: C, XXX; H, XXX; N, XXX. **19**: Yield: 96%. ³¹P{¹H} NMR: 43.0. ¹H NMR: 8.99 (ddd, ³J_{HH} = 8 Hz, ³J_{PH} = 13 Hz, ⁴J_{HH} = 1 Hz, 1H, Ph); 7.29 (tdd, ³J_{HH} = 8 Hz, ⁴J_{PH} = 1 Hz, ⁴J_{HH} = 1 Hz, 1H, Ph); 7.1–6.9 (m, 6H, Ph, Ph); 6.83 (ddd, ³J_{HH} = 8 Hz, ⁴J_{PH} = 5 Hz, ⁴J_{HH} = 1 Hz, 1H, Ph); 2.20 (s, 15 H, Cp*); 1.13 (d, ³J_{PH} = 16 Hz, 18 H, *t*-Bu). ¹³C{¹H} NMR: 144.1, 139.3 (d, ²J_{CP} = 7 Hz), 133.2 (d, ⁴J_{CP} = 10 Hz), 130.8, 130.7, 128.2, 127.6, 126.9 (d, ³J_{CP} = 10 Hz), 125.6 (s, Cp*), 40.4 (d, ¹J_{CP} = 51 Hz), 28.3 (s, *t*-Bu); 13.2 (s, Cp*). Anal. Calcd for C₃₀H₄₂Cl₂NPTi: C, 72.7; H, 8.5; N, 2.8. Found: C, 72.5; H, 8.3; N, 2.6.

Synthesis of CpTi(NP*t*-Bu₂(2-C₆H₄Ph)), **20.** A 5 mL sample of ether was added to a mixture of 225 mg (0.479 mmol) of compound **18** and 70 mg (2.879 mmol) of Mg powder. Then 150 μL of THF was added dropwise, and the mixture was stirred vigorously for 5 days. The solvent was then removed in vacuo and the residue extracted repeatedly with pentane; the extracts were filtered through Celite, after which the solvent was removed. Yield: 60%. ³¹P{¹H} NMR: 18.6. ¹H NMR: 7.54 (m, 1H, C₆H₄); 7.07 (m, 1H, C₆H₄); 7.02 (m, 1H, C₆H₄); 6.78 (m, 1H, C₆H₄); 6.22 (m, 5H, Cp); 4.53 (m, 2H, *o*-Ph); 4.40 (m, 2H, *m*-Ph); 3.48 (m, 1H, *p*-Ph); 0.96 (d, ³J_{PH} = 13.7 Hz, 27H, *t*-Bu). ¹³C{¹H} NMR: 148.8 (d, J_{PC} = 6 Hz), 131.9 (m, J_{PC} = 58), 131.3 (d, J_{PC} = 8 Hz), 130.2 (d, J_{PC} = 7 Hz), 130.1, 125.6 (d, J_{PC} = 9 Hz), 125.1, 118.8, 104.0, 103.8, 100.2, 37.0 (d, J_{PC} = 61.0 Hz), 28.6. Anal. Calcd for C₂₅H₃₂NPTi: C, 70.6; H, 7.6; N, 3.3. Found: C, 70.4; H, 7.3; N, 3.0.

Synthesis of Cp*Ti(NP*t*-Bu₂(2-C₆H₄Ph)), **21.** A solution of **19** (805 mg, 1.622 mmol) in 10 mL of THF was added dropwise to 200 mg (8.227 mmol) of Mg powder in 10 mL of THF at –80 °C. The solution was warmed to 25 °C and stirred for 90 min, over which time it turned red-brown. The solvent was removed in vacuo, and the residue was extracted with 5 × 5 mL of pentane. The extracts were filtered, and the solvent was removed in vacuo. Yield: 31% of a red-brown solid. **21**: ³¹P{¹H} NMR: 18.6. ¹H NMR: 7.57 (m, 1H, C₆H₄); 7.17 (m, 1H, C₆H₄); 7.01 (m, 1H, C₆H₄); 6.78 (m, 1H, C₆H₄); 4.42 (m,

2H, Ph); 4.27 (m, 2H, m, 2H, Ph); 3.65 (m, 1H, m, 2H, Ph); 1.99 (s, 15H, Cp*); 1.02 (d, ³J_{PH} = 7 Hz, 27H, *t*-Bu). ¹³C{¹H} NMR: 149.6 (d, J_{PC} = 7 Hz), 133.6 (d, J_{PC} = 55 Hz), 133.1 (d, J_{PC} = 8 Hz), 129.4, 129.4, 125.3, 124.9 (d, J_{PC} = 4 Hz), 124.6 (d, J_{PC} = 8 Hz), 117.4, 114.5, 104.4, 101.4, 37.3 (d, ¹J_{PC} = 61 Hz), 29.2, 13.7. Anal. Calcd for C₃₀H₅₂NPTi: C, 71.3; H, 10.4; N, 2.8. Found: C, 70.9; H, 10.3; N, 2.5.

Synthesis of Cp*Ti(NP*t*-Bu₃)(CO)₂, **22.** A solution of 230 mg (0.489 mmol) of **11** in 5 mL of THF was added dropwise at –80 °C to 100 mg (4.114 mmol) of Mg powder in 5 mL of THF in a 200 mL glass vessel. The mixture was frozen and degassed by two freeze–pump–thaw cycles, and then CO was admitted at –80 °C to atmospheric pressure. The vessel was sealed, and the solution was warmed slowly to room temperature with vigorous stirring. After stirring overnight, the solvent was then removed in vacuo and the residue was extracted repeatedly with pentane (ca. 5 × 10 mL). The extracts were filtered through Celite, and the solvent was removed in vacuo to give 157 mg (70%) of a green crystalline product. X-ray quality crystals may be obtained by recrystallization of the material from ether at –35 °C. ³¹P{¹H} NMR: 34.2. ¹H NMR: 1.60 (s, 15H, Cp*); 1.08 (d, ³J_{PH} = 13 Hz, 27H, *t*-Bu). ¹³C NMR (partial): 109.2, 40.1 (d, ¹J_{PC} = 45.8 Hz), 29.8, 12.0. IR: ν_{CO} (pentane solution, cm^{–1}) 1948, 1840. Anal. Calcd for C₂₄H₄₂NO₂PTi: C, 63.3; H, 9.3; N, 3.1. Found: C, 63.1; H, 9.6; N, 3.5.

X-ray Data Collection and Reduction. Crystals were manipulated and mounted in capillaries in a glovebox, thus maintaining a dry, O₂-free environment for each crystal. Diffraction experiments were performed on a Siemens SMART System CCD diffractometer. The data were collected in a hemisphere of data in 1329 frames with 10 s exposure times. The observed extinctions were consistent with the space groups in each case. The data sets were collected (4.5° < 2θ < 45–50.0°). A measure of decay was obtained by re-collecting the first 50 frames of each data set. The intensities of reflections within these frames showed no statistically significant change over the duration of the data collections. The data were processed using the SAINT and XPREP processing packages. An empirical absorption correction based on redundant data was applied to each data set. Subsequent solution and refinement were performed using the SHELXTL solution package.

Structure Solution and Refinement. Non-hydrogen atomic scattering factors were taken from the literature tabulations.¹² The heavy atom positions were determined using direct methods employing the SHELXTL direct methods routine. The remaining non-hydrogen atoms were located from successive difference Fourier map calculations. The refinements were carried out by using full-matrix least-squares techniques on *F*, minimizing the function $w(|F_o| - |F_c|)^2$ where the weight *w* is defined as $4F_o^2/2\sigma(F_o^2)$ and *F*_o and *F*_c are the observed and calculated structure factor amplitudes. In the final cycles of each refinement, all non-hydrogen atoms were assigned anisotropic temperature factors in the absence of disorder or insufficient data. In the latter cases atoms were treated isotropically. C–H atom positions were calculated and allowed to ride on the carbon to which they are bonded assuming a C–H bond length of 0.95 Å. H atom temperature factors were fixed at 1.10 times the isotropic temperature factor of the C atom to which they are bonded. The H atom contributions were calculated, but not refined. The locations of the largest peaks in the final difference Fourier map calculation as well as the magnitude of the residual electron densities in each case were of no chemical significance. Additional details are provided in the Supporting Information.

Results and Discussion

Dimeric Ti(III) Complexes. The reduction of titanium phosphinimide complexes by Mg has been inves-

(12) Cromer, D. T.; Mann, J. B. *Acta Crystallogr. A* **1968**, *A24*, 321–324.

Table 1. Crystallographic Data

	4•0.5C ₆ H ₆	6	7•0.5(PhC) ₂	9	10	15
formula	C ₃₁ H ₅₅ Cl ₂ N ₂ P ₂ Ti ₂	C ₂₃ H ₄₂ NPTi	C ₅₂ H ₅₇ NPTi	C ₂₅ H ₄₇ NPSi ₂ Ti	C ₂₁ H ₄₀ NPTi	C ₂₃ H ₄₄ NPTi
fw	684.41	411.45	774.86	496.69	335.41	413.46
cryst syst	monoclinic	monoclinic	monoclinic	orthorhombic	monoclinic	triclinic
space group	<i>P2₁/c</i>	<i>P2₁/n</i>	<i>P2₁/c</i>	<i>Pnma</i>	<i>P2₁/c</i>	<i>P1</i>
<i>a</i> (Å)	17.100(8)	11.5454(12)	13.673(8)	17.654(10)	14.704(8)	8.398(2)
<i>b</i> (Å)	11.452(5)	15.1684(16)	10.905(7)	15.355(9)	19.551(11)	10.683(3)
<i>c</i> (Å)	19.780(10)	13.9632(14)	30.72(2)	11.611(6)	16.030(8)	14.425(4)
α (deg)	90	90	90	90	90	92.977(6)
β (deg)	114.213(8)	107.109(3)	90.861(12)	90	92.247(11)	97.380(6)
γ (deg)	90	90	90	90	90	106.036(6)
<i>V</i> (Å ³)	3533(3)	2337.1(4)	4580(5)	3147(3)	4605(4)	1228.3(6)
<i>Z</i>	4	4	4	4	8	2
<i>d</i> (calc) (g cm ⁻¹)	1.287	1.169	1.124	1.048	1.112	1.118
abs coeff, μ (cm ⁻¹)	0.716	0.442	0.255	0.410	0.444	0.420
no. of data collected	14 517	7296	19 199	12 811	19 475	5058
data <i>F</i> _o ² > 3σ(<i>F</i> _o ²)	5054	2468	6547	2324	6546	3461
no. of variables	352	235	449	145	433	253
<i>R</i>	0.0320	0.0930	0.0645	0.0439	0.0569	0.0530
<i>R</i> _w	0.0869	0.1495	0.1465	0.1275	0.1524	0.1515
GOF	1.030	0.964	0.817	1.001	0.965	1.136

	17	18•0.5C ₆ H ₆	19•0.5C ₆ H ₆	20	21	22
formula	C ₂₃ H ₃₆ NPSi	C ₂₈ H ₃₅ Cl ₂ NPTi	C ₃₃ H ₄₅ Cl ₂ NP Ti	C ₂₅ H ₃₂ NPTi	C ₃₀ H ₄₂ NPTi	C ₁₄ H ₄₂ NO ₂ PTi
fw	385.59	535.34	605.47	425.39	495.56	455.46
cryst syst	monoclinic	triclinic	monoclinic	monoclinic	monoclinic	orthorhombic
space group	<i>Cc</i>	<i>P1</i>	<i>P2₁/n</i>	<i>P2₁/n</i>	<i>P2₁/c</i>	<i>Pna2₁</i>
<i>a</i> (Å)	15.861(13)	10.394(6)	12.409(7)	9.370(5)	20.261(19)	20.510(10)
<i>b</i> (Å)	12.409(10)	11.240(7)	19.664(11)	20.591(12)	9.274(9)	8.536(4)
<i>c</i> (Å)	12.468(10)	12.855(8)	14.132(7)	12.046(7)	29.54(3)	15.276(8)
α (deg)	90	81.526(10)	90	90	90	90
β (deg)	102.927(14)	77.385(10)	100.792(11)	100.181(11)	91.409(17)	90
γ (deg)	90	88.547(11)	90	90	90	90
<i>V</i> (Å ³)	2392(3)	1449.4(14)	3388(3)	2288(2)	5548(9)	2675(2)
<i>Z</i>	4	2	4	4	8	4
<i>d</i> (calc) (g cm ⁻¹)	1.071	1.227	1.187	1.235	1.186	1.131
abs coeff, μ (cm ⁻¹)	0.172	0.550	0.479	0.454	0.384	0.397
no. of data collected	4950	6229	14 263	9752	19 011	10 795
no. of data <i>F</i> _o ² > 3σ(<i>F</i> _o ²)	3253	4144	4803	3289	7715	3737
no. of variables	235	283	336	253	595	262
<i>R</i>	0.0330	0.0561	0.0412	0.0378	0.0591	0.0271
<i>R</i> _w	0.0829	0.1665	0.1076	0.0851	0.1406	0.0636
GOF	1.008	1.057	0.867	0.853	0.871	0.923

tigated. Reaction of the simple phosphinimide complexes CpTi(NPR₃)Cl₂ (R = Me **1**, *i*-Pr **2**) with Mg in THF afforded complexes formulated as [CpTiCl(μ-NPR₃)₂] (R = Me **3**, *i*-Pr **4**). In the case of **4** crystals were obtained and the resulting crystallographic data confirmed the dimeric formulation in which the phosphinimide ligands bridge the two metal centers (Figure 1). The cyclopentadienyl ligands adopt a *cisoid* conformation, while a chloride ligand completes the coordination sphere of each of the Ti centers. The Ti–N and Ti–Cl distances average 2.014(2) and 2.3819(12) Å, respectively. The Ti–N–Ti and N–Ti–N angles within the Ti₂N₂ core average 82.60(8)° and 93.37(8)°, respectively, affording a Ti–Ti separation of 2.6612(10) Å. The Ti–N distances of 2.013(2) and 2.024(2) Å and the average P–N–Ti angles of 137.48(12)°, 139.14(13)°, 139.53(12)°, and 137.27(13)° reflect the slight dissymmetry of the bridging phosphinimide core. It is particularly noteworthy that the structure of **4** stands in contrast to that previously reported for the chloro-bridged Ti(III) dimer [CpTi(NP*t*-Bu₃)(μ-Cl)]₂ (Scheme 1), derived from reduction of CpTi(NP*t*-Bu₃)Cl₂ (**5**) with Mg in benzene.⁹ This dramatic structural difference for these Ti(III) species is attributed to the greater steric demands of the *t*-Bu₃PN ligand. A related Ti(III)-phosphinimide-bridged species, [TiBr₂(μ-NPPH₃)₂], has been previously de-

scribed by Dehnicke et al. In this species the Ti–N and Ti···Ti separations are somewhat shorter than in **3**.¹³

Ti(IV) Metallacycles. In contrast to the above chemistry, CpTi(NP*t*-Bu₃)Cl₂ (**5**) is reduced by Mg to a putative Ti(II) species when the reduction is performed in THF. This intermediate can be intercepted by reaction with a variety of reagents to give monometallic, metallacyclic complexes. In the case of reduction in the presence of 2,3-dimethyl-1,3-butadiene, the very sensitive species CpTi(NP*t*-Bu₃)(CH₂C(Me)C(Me)CH₂) (**6**) is obtained in 85% yield. This species exhibited a single resonance in the ³¹P{¹H} NMR spectrum, and the ¹H and ¹³C{¹H} NMR data were consistent with the above formulation. Both *cis* and *trans* conformations of the butadiene as well as prone and supine isomers (Scheme 2), in which only the orientation of the butadiene ligand with respect to the cyclopentadienyl ligands differs, are conceivable. At ambient temperature, two doublets of equal intensity attributable to the terminal CH₂ of the diene are observed in the ¹H NMR spectrum of **6**. The lower and higher field resonances of these were assigned to the *syn* and *anti* protons, respectively. A NOESY NMR experiment shows a correlation between the methyl protons and the Cp protons, which suggests that

(13) Li, J.-s.; Weller, F.; Schmock, F.; Dehnicke, K. *Z. Anorg. Allg. Chem.* **1995**, *621*, 2097–2103.

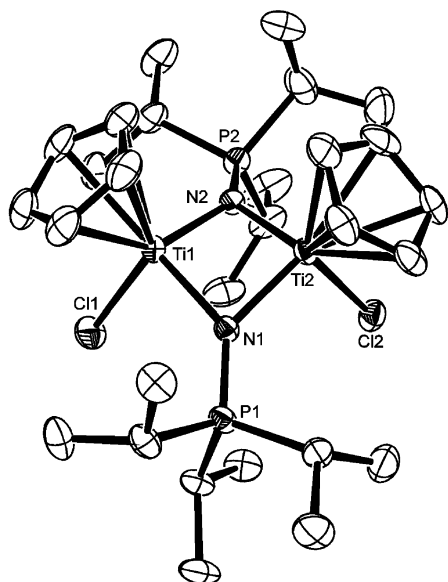
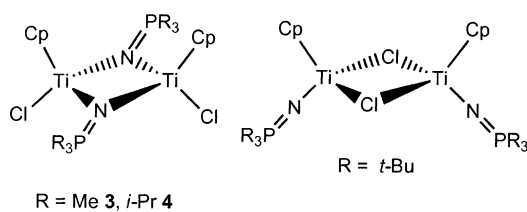
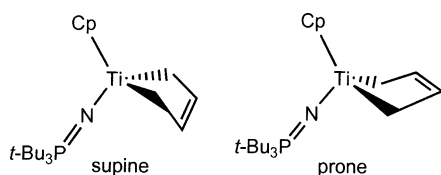


Figure 1. ORTEP drawings of **4**, 30% thermal ellipsoids are shown. Hydrogen atoms are omitted for clarity. Distances (Å) angles (deg): Ti(1)–N(2) 2.011(2), Ti(1)–N(1) 2.017(2), Ti(1)–Cl(1) 2.3806(12), Ti(1)–Ti(2) 2.6612(10), Ti(2)–N(1) 2.013(2), Ti(2)–N(2) 2.024(2), Ti(2)–Cl(2) 2.3832(14), P(1)–N(1) 1.617(2), P(2)–N(2) 1.612(2), N(2)–Ti(1)–N(1) 93.51(9), N(2)–Ti(1)–Cl(1) 105.39(7), N(1)–Ti(1)–Cl(1) 95.12(7), N(1)–Ti(2)–N(2) 93.24(8), N(1)–Ti(2)–Cl(2) 104.55(7), N(2)–Ti(2)–Cl(2) 96.38(7), P(1)–N(1)–Ti(1) 137.48(12), P(1)–N(1)–Ti(2) 139.14(13), Ti(1)–N(1)–Ti(2) 82.67(8), P(2)–N(2)–Ti(1) 139.53(12), P(2)–N(2)–Ti(2) 137.27(13), Ti(1)–N(2)–Ti(2) 82.53(8).

Scheme 1



Scheme 2



the butadiene fragment is in the prone configuration. The ¹³C{¹H} NMR spectrum displays resonances at 116.3 and 62.4 ppm for the internal and terminal diene carbon atoms, respectively. This significant chemical shift difference between the two carbon atoms is in accord with a substantial σ -complex character in the conjugated diene, which supports a Ti(IV) formulation. The precise nature of **6** was unambiguously confirmed via X-ray crystallography (Figure 2). These data reveal coordination of *cis*-butadiene ligands, such that the butadiene substituents are oriented toward the cyclopentadienyl ligand. This orientation presumably avoids unfavorable steric interactions between the butadiene-methyl substituents and the phosphinimide ligand. The phosphinimide ligand geometry is approximately linear

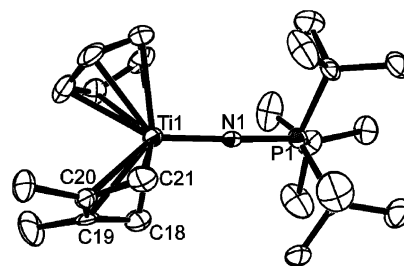


Figure 2. ORTEP drawings of **6**, 30% thermal ellipsoids are shown. Hydrogen atoms are omitted for clarity. Distances (Å) angles (deg): Ti(1)–N(1) 1.852(9), Ti(1)–C(21) 2.141(11), Ti(1)–C(18) 2.157(11), Ti(1)–C(20) 2.409(12), Ti(1)–C(19) 2.417(11), P(1)–N(1) 1.558(9), C(18)–C(19) 1.450(16), C(19)–C(20) 1.398(16), C(19)–C(22) 1.523(15), C(20)–C(21) 1.441(15), C(20)–C(23) 1.540(16), C(21)–Ti(1)–C(20) 36.3(4), C(18)–Ti(1)–C(20) 66.2(5), N(1)–Ti(1)–C(19) 127.7(4), C(21)–Ti(1)–C(19) 65.3(5), C(18)–Ti(1)–C(19) 36.4(4), C(20)–Ti(1)–C(19) 33.7(4), P(1)–N(1)–Ti(1) 178.0(6), C(19)–C(18)–Ti(1) 81.6(7), C(20)–C(19)–C(18) 122.8(12), C(20)–C(19)–Ti(1) 72.9(7), C(18)–C(19)–Ti(1) 62.0(6), C(19)–C(20)–C(21) 121.0(12), C(19)–C(20)–Ti(1) 73.5(7), C(20)–C(21)–Ti(1) 82.0(7).

at N, although the Ti–N distance of 1.852(9) Å is significantly longer than that seen in the related dichloride or dialkyl complexes. The Ti–C distances for the α - and β -butadiene carbon atoms average 2.149(11) and 2.413(11) Å, while the C–C distances of the central bond of the butadiene ligand are 1.398(16) Å. These data suggest that **6** may be described as a Ti(IV) species in which the butadiene is best bound via a σ^2 , π -bonded η^4 -interaction. The structural parameters of the butadiene moieties are typical of those seen for a number of other early metal butadiene complexes.^{14–16} and as well as the constrained geometry derivative (C₅Me₄SiMe₂N*t*-Bu)Ti(CH₂C(Me)C(Me)CH₂).¹⁷

In a similar manner, the reduction of **5** in the presence of diphenylacetylene gave the species CpTi(NP*t*-Bu₃)(C₂Ph₂)₂ (**7**) in 70% yield. While NMR data are consistent with the diphenylacetylene-to-Ti ratio, X-ray data were required to determine the structure (Figure 3). These data confirm the metallocyclopentadiene structure, in which reductive coupling of two acetylene units has occurred to form the five-membered ring. The structural parameters of the CpTi(NP*t*-Bu₃) fragment are similar to that observed in **6**. However, the central C β –C β bond length of the metallocyclopentadiene portion of the molecule (1.502(7) Å) is significantly longer than the other two C–C bonds in the metallacycle (1.396(7), 1.355(7) Å). These data support the formulation of **7** as a Ti(IV) species. The related reaction of phenylacetylene affords a similar metallacyclic product, CpTi(NP*t*-Bu₃)(CPhCHCPhCH) (**8**), in good yield. NMR data indicate a head-to-tail coupling, with the non-equivalent vinylic C–H resonances appearing at 8.05 and 7.58 ppm in the ¹H NMR spectrum. This orientation presumably results in lower steric congestion. The

(14) Dorf, U.; Engel, K.; Erker, G. *Organometallics* **1983**, *2*, 462–463.

(15) Beckhaus, R.; Thiele, K. H. *J. Organomet. Chem.* **1986**, *317*, 23–31.

(16) Yamamoto, H.; Yasuda, H.; Tatsumi, K.; Lee, K.; Nakamura, A.; Chen, J.; Kai, Y.; Kasai, N. *Organometallics* **1989**, *8*, 105–119.

(17) Devore, D. D.; Timmers, F. J.; Hasha, D. L.; Rosen, R. K.; Marks, T. J.; Deck, P. A.; Stern, C. L. *Organometallics* **1995**, *14*, 3132–3134.

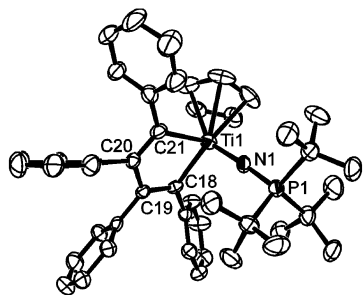
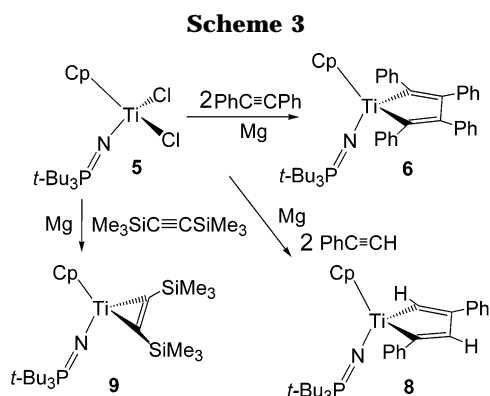


Figure 3. ORTEP drawings of **7**, 30% thermal ellipsoids are shown. Hydrogen atoms are omitted for clarity. Distances (Å) angles (deg): Ti(1)–N(1) 1.796(5), Ti(1)–C(18) 2.138(6), Ti(1)–C(21) 2.153(6), P(1)–N(1) 1.609(5), C(18)–C(19) 1.396(7), C(19)–C(20) 1.502(7), C(20)–C(21) 1.355(7), N(1)–Ti(1)–C(18) 104.8(2), N(1)–Ti(1)–C(21) 104.3(2), C(18)–Ti(1)–C(21) 82.9(2), P(1)–N(1)–Ti(1) 175.3(3), C(19)–C(18)–Ti(1) 108.8(4), C(22)–C(18)–Ti(1) 128.5(4), C(18)–C(19)–C(20) 117.8(5), C(21)–C(20)–C(19) 120.2(5), C(20)–C(21)–Ti(1) 109.0(4).



analogous regiochemistry has been described for the thermodynamically favored isomer of $\text{CpTi}(\text{OC}_6\text{HPh}_4)\text{-}((t\text{-Bu})\text{CCHC}(t\text{-Bu})\text{CH})$ and $\text{Cp}_2\text{Ti}((t\text{-Bu})\text{CCHC}(t\text{-Bu})\text{CH})$.¹⁸ An analogous reaction with bis(trimethylsilyl)acetylene resulted in the formation of the species $\text{CpTi}(\text{NP}t\text{-Bu}_3)(\eta^2\text{-C}_2(\text{SiMe}_3)_2)$ (**9**) (Scheme 3). Structural data confirmed the 2-fold symmetry of this titanacyclopentene molecule (Figure 4). The Ti–C bond length for the η^2 -acetylene fragment is 2.062(3) Å. The corresponding bond lengths of 2.125(3) and 2.144(3) Å reported for $(\text{C}_5\text{Me}_4\text{SiMe}_3)_2\text{Ti}(\eta^2\text{-C}_2(\text{SiMe}_3)_2)$ ¹⁹ are longer than those in **9**, consistent with the presence of the electron-donating Cp ligand. The C–C bond length of 1.314(6) Å is indicative of back-donation to the acetylene ligand and suggests a Ti(IV)-metallacyclic structure. Nonetheless, a Ti(II) formulation is suggested by literature precedent of the related species $\text{Cp}'_2\text{Ti}(\eta^2\text{-C}_2(\text{SiMe}_3)_2)$. These metallocene analogues have been shown to be effective synthons for a variety of titanocene derivatives as a result of the lability of the acetylene.^{20,21}

The reduction of **5** in the presence of ethylene affords the compound $\text{CpTi}(\text{NP}t\text{-Bu}_3)(\text{CH}_2)_4$ (**10**), in which two ethylene ligands have been reductively coupled to form

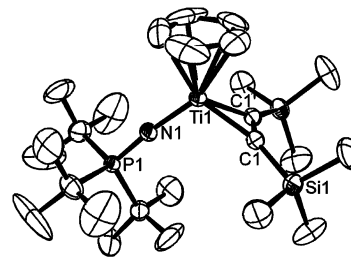


Figure 4. ORTEP drawings of **9**, 30% thermal ellipsoids are shown. Hydrogen atoms are omitted for clarity. Distances (Å) angles (deg): Ti(1)–N(1) 1.842(3), Ti(1)–C(1) 2.062(3), Ti(1)–C(1') 2.062(3), C(1)–C(1') 1.314(6), P(1)–N(1) 1.575(3), N(1)–Ti(1)–C(1) 109.06(12), N(1)–Ti(1)–C(1') 109.06(12), C(1)–Ti(1)–C(1') 37.14(16), P(1)–N(1)–Ti(1) 173.5(2).

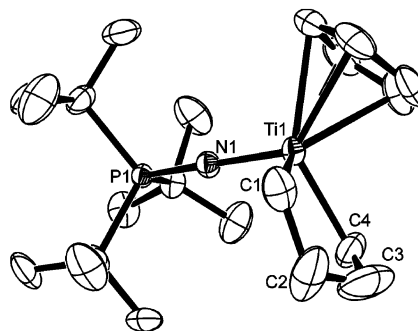


Figure 5. ORTEP drawings of one of the two molecules of **10** in the asymmetric unit, 30% thermal ellipsoids are shown. Hydrogen atoms are omitted for clarity. Distances (Å) angles (deg): Ti(1)–N(1) 1.813(3), Ti(1)–C(4) 2.131(5), Ti(1)–C(1) 2.155(6), P(1)–N(1) 1.583(3), N(1)–Ti(1)–C(4) 104.71(19), N(1)–Ti(1)–C(1) 105.7(2), C(4)–Ti(1)–C(1) 86.2(3), C(2)–C(1)–Ti(1) 101.9(5), C(3)–C(2)–C(1) 114.7(7), C(2)–C(3)–C(4) 116.8(8), C(3)–C(4)–Ti(1) 103.0(5).

a five-membered ring. The ¹H NMR spectrum shows diastereotopic α -H resonances appearing at 2.58 and 2.18 ppm, and the β -H signals, which are coincidentally degenerate, appear at 1.75 ppm. The X-ray structure for **10** reveals the Ti–C bond lengths in the two molecules in the asymmetric unit range from 2.130(6) to 2.155(6) Å (Figure 5). The $\text{C}_\alpha\text{-C}_\alpha$ bond distances within the TiC_4 rings are typical of C–C single bonds. The $\text{C}_\beta\text{-C}_\beta$ bond lengths were found to be 1.373(12) and 1.388(13) Å. These unexpectedly short C–C bonds are thought to reflect some disorder of these carbon positions, although efforts to model such a disorder were unsuccessful. Nonetheless, the structural data indicate a Ti(IV) formulation. In a manner similar to that used for the synthesis of **10**, the species $\text{Cp}^*\text{Ti}(\text{NP}t\text{-Bu}_3)(\text{CH}_2)_4$ (**12**) and (indenyl) $\text{Ti}(\text{NP}t\text{-Bu}_3)(\text{CH}_2)_4$ (**14**) were prepared from **11** and **13**, respectively.

The analogous reaction of **5** with propylene afforded the complex formulated as $\text{CpTi}(\text{NP}t\text{-Bu}_3)(\text{CH}_2\text{CHMe})_2$ (**15**). ¹H and ¹³C{¹H} NMR data were consistent with the formation of only the meso diastereomers (Figure 6) in which both methyl groups reside on the carbon atoms β to the metal center. X-ray data for **15** confirmed this formulation (Figure 7), although the data also revealed the disorder of the β -carbon positions. The metric parameters were similar to those observed for **10** as expected. The formation of the isomer of the 3,4-dimethyltitanacyclopentane **15** stands in contrast to the

(18) Lee, J.; Fanwick, P. E.; Rothwell, I. P. *Organometallics* **2003**, *22*, 1546.

(19) Horacek, M.; Kupfer, V.; Thewalt, U.; Stepnicka, P.; Polasek, M.; Mach, K. *Organometallics* **1999**, *18*, 3572–3578.

(20) Rosenthal, U.; Burlakov, V. V.; Arndt, P.; Baumann, W.; Spannenberg, A. *Organometallics* **2003**, *22*, 884–900.

(21) Rosenthal, U.; Pellny, P.-M.; Kirchbauer, F. G.; Burlakov, V. *Acc. Chem. Res.* **2000**, *33*, 119–129.

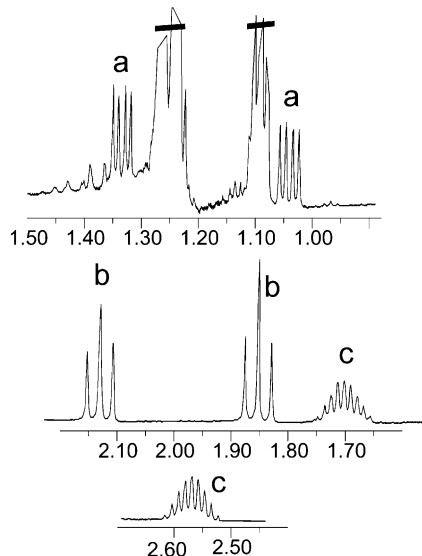


Figure 6. ^1H NMR spectrum of the methylene (a, b) and methine (c) protons of **15**.

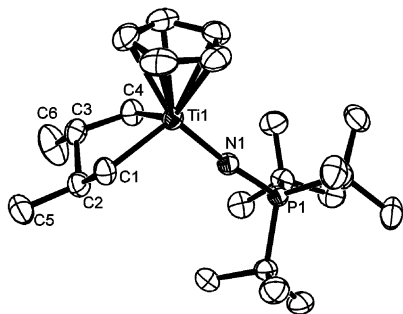
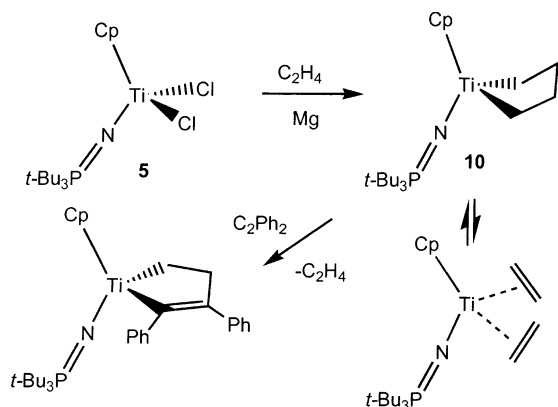


Figure 7. ORTEP drawings of **15**, 30% thermal ellipsoids are shown. One of the two disordered positions of C(2) and C(3) is shown. Hydrogen atoms are omitted for clarity. Distances (Å) angles (deg): Ti(1)–N(1) 1.804(2), Ti(1)–C(1) 2.146(3), Ti(1)–C(4) 2.150(3), N(1)–Ti(1)–C(1) 105.45(12), N(1)–Ti(1)–C(4) 104.71(13), P(1)–N(1)–Ti(1) 171.39(16).

Scheme 4



2,4-substitution pattern seen in **8**. This is attributable to additional steric crowding that results in the planar titanacyclopentadiene ring of **8**.

The isolation and characterization of **10**, **12**, **14**, and **15** stand in contrast to the isolation of $\text{Cp}^*_2\text{Ti}(\text{C}_2\text{H}_4)$ and the instability of $\text{Cp}^*_2\text{Ti}(\text{CH}_2)_4$, described by Bercaw et al.^{22,23} The presence of the phosphinimide ligand appears to provide room at the metal, thus stabilizing the bis-ethylene species. Nonetheless, reactions of **10** re-

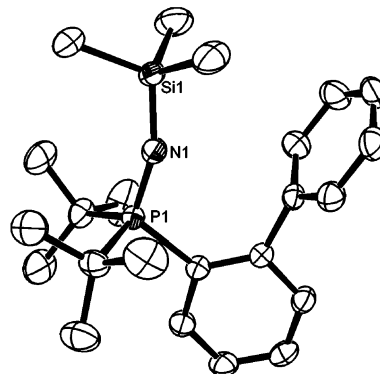


Figure 8. ORTEP drawings of **17**, 30% thermal ellipsoids are shown. Hydrogen atoms are omitted for clarity. Distances (Å) angles (deg): P(1)–N(1) 1.531(2), Si(1)–N(1) 1.674(2), P(1)–N(1)–Si(1) 160.76(15).

vealed that the Ti(IV) formulation is a simplistic view and that like the Cp^* -analogue, the C–C bond formation is readily reversible. For example, **10** reacts with PhCCPh to generate the species $\text{CpTi}(\text{NP}t\text{-Bu}_3)(\text{CH}_2)_2\text{-}(\text{CPh})_2$ (**16**), via the putative Ti(II) species $\text{CpTi}(\text{NP}t\text{-Bu}_3)(\text{C}_2\text{H}_4)_2$ (Scheme 4). This suggests that **10** could be useful as a Ti(II) synthon.

Intramolecular Ti(IV) Metallacycles. In an attempt to effect intramolecular metalation, an analogous complex incorporating a pendant biphenyl group was prepared. This effort began with the conventional oxidation of $Pt\text{-Bu}_2(2\text{-C}_6\text{H}_4\text{Ph})$ with N_3SiMe_3 , which afforded the phosphinimine $t\text{-Bu}_2(2\text{-C}_6\text{H}_4\text{Ph})\text{PNSiMe}_3$ (**17**)⁵ after a two week period at reflux. In contrast, $t\text{-Bu}_3\text{P}$ is completely oxidized with N_3SiMe_3 after several hours at 90 °C. The resistance to oxidation of the biphenylphosphine is evidence of the crowding provided by the biphenyl substituent, and X-ray data for **17** (Figure 8) show the orientation of the biphenyl substituent is toward the NSiMe_3 fragment. Employing literature methods, the Ti complexes $\text{Cp}'\text{Ti}(t\text{-Bu}_2(2\text{-C}_6\text{H}_4\text{Ph})\text{PN})\text{-Cl}_2$ ($\text{Cp}' = \text{Cp}$ **18**, Cp^* **19**) were prepared from reaction of the **17** with $\text{Cp}'\text{TiCl}_3$ in yields of 89 and 96%, respectively.⁵ Subsequently, crystallographic data for **18** and **19** (Figure 9) revealed similar Ti–N distances of 1.759(3) and 1.791(3) Å, respectively, and P–N distances of 1.619(3) and 1.609(3) Å. For **19**, the slightly longer Ti–N distance and shorter P–N bond length are consistent with greater electron donation from Cp^* . The P–N–Ti angles in **18** and **19** are approximately linear at 177.0(2)° and 172.71(16)°, respectively, typical of terminal phosphinimide ligand complexes.¹ $^{31}\text{P}\{^1\text{H}\}$, ^1H , and $^{13}\text{C}\{^1\text{H}\}$ NMR data revealed the presence of two isomers in a ratio of 3:1 for **18** and a single isomer for **19**. These data imply inhibited rotation of the biphenyl substituents (Scheme 5). This view is consistent with the observation of only a single isomer of **19**, where the increased steric demands of the Cp^* ligand preclude rotation about the P–C(biphenyl) bond. The relatively poor solubility of **18** precluded a determination of the rotational barrier.

Reduction of **18** and **19** with Mg in THF/ Et_2O proceeds cleanly to give red-brown products, formulated as

(22) Cohen, S. A.; Auburn, P. R.; Bercaw, J. E. *J. Am. Chem. Soc.* **1983**, *4*, 1136.

(23) Cohen, S. A.; Bercaw, J. E. *Organometallics* **1985**, *4*, 1006–1014.

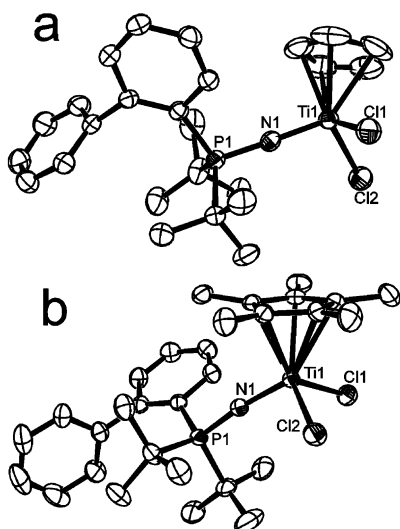


Figure 9. ORTEP drawings of (a) **18** and (b) **19**, 30% thermal ellipsoids are shown. Hydrogen atoms are omitted for clarity. Distances (Å) angles (deg): **18**: Ti(1)–N(1) 1.759(3), Ti(1)–Cl(1) 2.3087(17), Ti(1)–Cl(2) 2.3139(16), P(1)–N(1) 1.619(3), N(1)–Ti(1)–Cl(1) 102.62(11), N(1)–Ti(1)–Cl(2) 102.19(10), Cl(1)–Ti(1)–Cl(2) 101.73(7), P(1)–N(1)–Ti(1) 177.0(2). **19**: Ti(1)–N(1) 1.791(3), Ti(1)–Cl(2) 2.3091(13), Ti(1)–Cl(1) 2.3219(14), N(1)–P(1) 1.609(3), N(1)–Ti(1)–Cl(2) 102.70(9), N(1)–Ti(1)–Cl(1) 102.84(9), Cl(2)–Ti(1)–Cl(1) 101.23(5), P(1)–N(1)–Ti(1) 172.71(16).

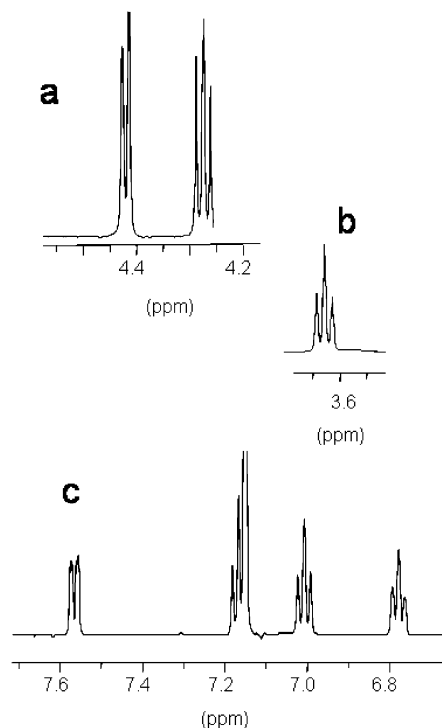
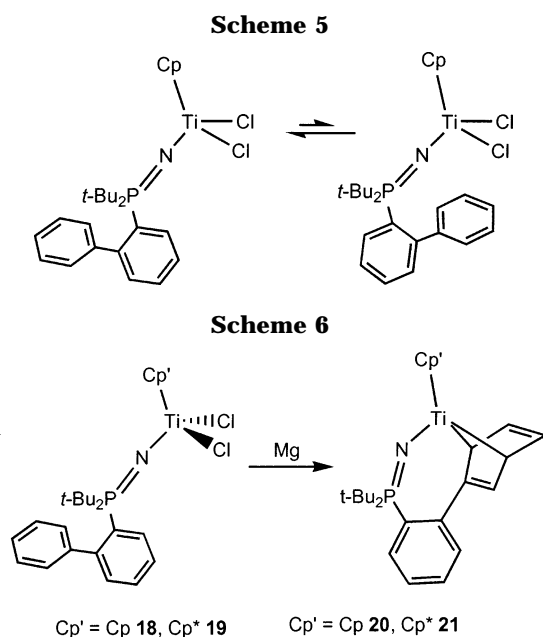


Figure 10. ^1H NMR spectrum of arene protons of the Ti–arene interaction in **20**.



$[\text{Cp}'\text{Ti}(\text{NP}t\text{-Bu}_2(2\text{-C}_6\text{H}_4\text{Ph}))]$ (Cp' = Cp **20**, Cp* **21**) (Scheme 6). These products were isolated in 60 and 50% yields, respectively. NMR data were consistent with the presence of the Cp and phosphinimide ligand resonances in a 1:1 ratio in both cases. In the case of **20** resonances observed at 7.54, 7.07, 7.02, 6.78, 4.53, 4.40, and 3.48 ppm were attributed to biphenyl protons. Similar resonances were observed for the biphenyl protons of **21** (Figure 10). The dramatic upfield shift of phenyl protons to 4.42, 4.27, and 3.65 ppm (Figure 10a,b) and the well-separated phenyl protons at 7.57, 7.17, 7.01, and 6.78 ppm (Figure 10c) are consistent with a significant perturbation of one of the arene rings via interaction with the Ti center. X-ray crystals of **20** and **21** were

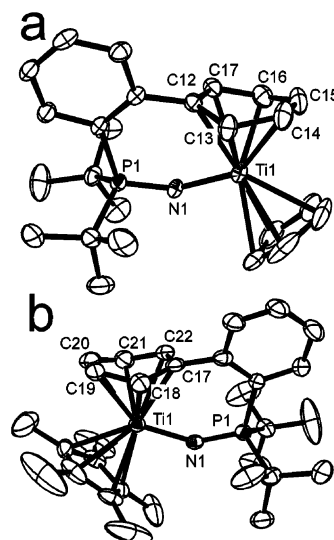


Figure 11. ORTEP drawing of (a) **20** and (b) **21** (one molecule from the asymmetric unit), 30% thermal ellipsoids are shown. Hydrogen atoms are omitted for clarity. Distances (Å) angles (deg): **20**: Ti(1)–N(1) 1.887(2), Ti(1)–C(12) 2.388(3), Ti(1)–C(13) 2.236(3), Ti(1)–C(14) 2.472(4), Ti(1)–C(15) 2.465(4), Ti(1)–C(16) 2.254(4), Ti(1)–C(17) 2.398(3), P(1)–N(1) 1.564(2), P(1)–N(1)–Ti(1) 145.3(2). **21**: Ti(1)–N(1) 1.918(4), Ti(1)–C(18) 2.236(5), Ti(1)–C(21) 2.242(6), Ti(1)–C(17) 2.397(5), Ti(1)–C(22) 2.416(5), Ti(1)–C(20) 2.447(7), Ti(1)–C(19) 2.456(6), P(1)–N(1) 1.557(4), P(1)–N(1)–Ti(1) 145.9(2).

obtained via recrystallization, and the solutions confirmed metal–arene interactions (Figure 11). The geometries about each of the Ti atoms are similar with coordination to the phosphinimide nitrogen atom, the η^5 -cyclopentadienyl ring, and η^6 -interaction with the pendant arene ring of the biphenyl substituent. The Ti–N distances in **20** and **21** average 1.887(2) and

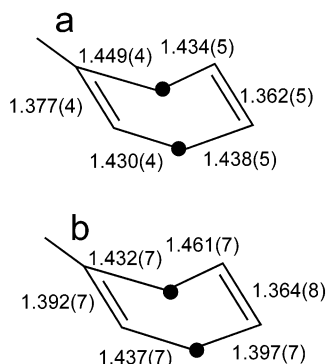


Figure 12. Ti–Arene interactions in (a) **20** and (b) **21**. Carbon atoms marked with ● are σ -bound to Ti.

1.913(4) Å, respectively, consistent with the greater electron donation to Ti in **21**. In contrast to **18** and **19**, the P–N–Ti angles in **20** and **21** are bent dramatically from linearity, being 145.3(2)° and 145.9(2)°, respectively. This angle is similar to the P–N–Ti angles seen for average doubly and triply bridging phosphinimide fragments in $[\text{Ti}_3\text{Cl}_6(\text{NPMe}_3)_5][\text{BPh}_4]$.²⁴ Presumably, the bend at N does not lead to dimerization or a bridging arrangement, as this atom resides in a rigid pocket which is sterically protected by the two *tert*-butyl groups on one side and the chelation of the biphenyl unit to Ti on the other.

The metric parameters associated with the η^6 -arene interactions suggest a reduction of the ring and thus a formal Ti(IV) formulation. The variations of the C–C bond lengths about the arene unit are consistent with a cyclohexadiene dianion resonance form (Figure 12). In **20**, the Ti–C(13) and Ti–C(16) distances of 2.236(3) and 2.254(4) Å are significantly shorter than the other Ti–C distance of the η^6 -arene, which range from 2.388(3) to 2.472(4) Å. Similarly in **21**, C(18) and C(21) are only 2.236(5) and 2.242(6) Å from Ti, while the remaining arene carbon atoms are between 2.398(5) and 2.454(6) Å from Ti. The result is a significant departure from planarity, as the dihedral angles through the close approach carbon atoms are 25.3° and 25.9° in **20** and **21**, respectively. This is consistent with the sp^3 character at C(13) and C(16) in **20** and C(18) and C(21) in **21** (Figure 12). Thus these species are best viewed as Ti(IV) metallacyclic species in which the arene ring is formally reduced. This geometry of the Ti–arene interaction is reminiscent of that seen in the Ti-bis-amidinate-toluene species described by Hagadorn and Arnold,²⁵ where similar bending of the arene ring gave rise to a dihedral angle of 20.0°.

Mechanistically, it is suggested that reduction of the Ti(IV)-dichlorides **18** and **19** generates transient Ti(II) species, which effects reduction of the arene unit and formal reoxidation of the metal to Ti(IV). Efforts to support this view via the interception of a Ti(II) intermediate with CO using the precursors **18** and **19** led instead to an inseparable mixture of products.

Ti(II) Species. In an effort to trap an unequivocal example of a Ti(II)-phosphinimide species, reductions were done in the presence of simple donor ligands. The

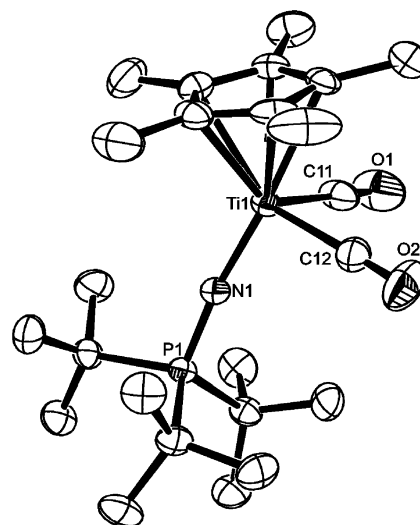


Figure 13. ORTEP drawings of one of the two molecules of **22** in the asymmetric unit, 30% thermal ellipsoids are shown. Hydrogen atoms are omitted for clarity. Distances (Å) angles (deg): Ti(1)–N(1) 1.841(2), Ti(1)–C12 2.021(3), Ti(1)–C11 2.028(4), Ti(1)–C5 2.341(3), Ti(1)–C(4) 2.352(3), Ti(1)–C(1) 2.366(3), Ti(1)–C(3) 2.403(3), Ti(1)–C(2) 2.413(3), P(1)–N(1) 1.586(2), C(11)–O(1) 1.150(4), C(12)–O(2) 1.146(3), N(1)–Ti(1)–C(12) 97.82(11), N(1)–Ti(1)–C(11) 100.42(11), C(12)–Ti(1)–C(11) 88.07(14), P(1)–N(1)–Ti(1) 172.30(14), O(1)–C(11)–Ti(1) 179.2(3), O(2)–C(12)–Ti(1) 178.1(3), N(1)–Ti(1)–C(12) 97.82(11), N(1)–Ti(1)–C(11) 100.42(11).

reduction of **5** in the presence of PMe_3 , $\text{Me}_2\text{PCH}_2\text{CH}_2\text{PMe}_2$, or nitriles afforded extremely sensitive products. Although preliminary spectral data suggested a fluxional Ti(II)-phosphine adduct, these compounds have not yet been fully characterized. The reduction of **5** in the presence of CO gave a mixture of products that could not be characterized. However, reduction of $\text{Cp}^*\text{Ti}(\text{NP}t\text{-Bu}_3)\text{Cl}_2$ (**11**) in the presence of CO resulted in the clean production of the green crystalline species $\text{Cp}^*\text{Ti}(\text{NP}t\text{-Bu}_3)(\text{CO})_2$ (**22**). IR stretching frequencies at 1948 and 1840 cm^{-1} were attributed to the coordinated CO. In comparison, the corresponding bands observed for $\text{Cp}_2\text{Ti}(\text{CO})_2$ (1977, 1899 cm^{-1})²⁶ and $\text{Cp}^*\text{Ti}(\text{CO})_2$ (1930, 1850 cm^{-1})²⁷ suggest that the phosphinimide ligand is a better electron donor than Cp, comparable to Cp^* . X-ray data confirmed the formulation of **22** as the unequivocal Ti(II)-phosphinimide derivative (Figure 13). The phosphinimide and carbonyl ligands are approximately linear. The Ti(1)–N(1) distance in **22** is 1.841(2) Å, which is significantly longer than the Ti–N bond distance seen in **5** (1.775(11) Å), presumably a result of the decreased electron donation from the phosphinimide ligand upon reduction from Ti(IV) to Ti(II). The Ti–C distances for the carbonyl groups were found to be 2.021(3) and 2.028(4) Å, while the C–O distances were 1.150(4) and 1.146(3) Å. These data are similar to those reported for $\text{Cp}_2\text{Ti}(\text{CO})_2$.²⁸ The N–Ti–C_{CO} angles of 97.82(11)° and 100.42(11)° and C_{CO}–Ti–C_{CO} angle of 88.07(14)° are significantly different from the

(26) Edwards, B. H.; Rogers, R. D.; Sikora, D. J.; Atwood, J. L.; Rausch, M. D. *J. Am. Chem. Soc.* **1983**, *105*, 416–426.

(27) Brintzinger, H.; Marvich, R. H. *J. Am. Chem. Soc.* **1971**, *93*, 2046–2048.

(28) Atwood, J. L.; Stone, K. E.; Alt, H. G.; Hrcncir, D. C.; Rausch, M. D. *J. Organomet. Chem.* **1975**, *96*, C4–C6.

(24) Ruebenstahl, T.; Weller, F.; Harms, K.; Dehnicke, K. *Z. Anorg. Allg. Chem.* **1994**, *620*, 1741–1749.

(25) Hagadorn, J. R.; Arnold, J. *Angew. Chem., Int. Ed.* **1998**, *37*, 1813–1815.

N–Ti–Cl and Cl–Ti–Cl angles of 102.6(2)°, 102.7(2)°, and 102.69(12)° of **5**, consistent with reduction of the Ti center.

Summary

The reduction chemistry described above illuminates several key points. The reduction of Cp-Ti-phosphinimide species with small phosphinimide substituents affords phosphinimide-bridged Ti(III) dimers. Surprisingly, further reduction of these dimeric species does not appear to occur readily. This stands in marked contrast to the reduction of **5**, where either chloro-bridged Ti(III) species⁹ or putative Ti(II) species are generated. The larger steric demands of the *t*-Bu₃PN ligand cause the redox chemistry of **5** and **11** to mimic that of titanocene, affording Ti(IV) cycloaddition products with olefins and acetylenes^{20,29} and the interception of a Ti(II) species with carbon monoxide. These results

also support the view that the ligand scaffold of CpTi(NP*t*-Bu₃) is a steric equivalent to Cp₂Ti, a concept that was previously employed in the design of phosphinimide-based olefin polymerization catalysts.^{4,10} The utility of the transient-phosphinimide Ti(II) species in a variety of applications is currently under investigation. The results of these efforts will be reported in due course.

Acknowledgment. Financial support from NSERC of Canada and NOVA Chemicals Corporation is gratefully acknowledged.

Supporting Information Available: Crystallographic data. This material is available free of charge via the Internet at <http://pubs.acs.org>.

OM049826Q

(29) Rosenthal, U.; Burlakov, V. V. *Titanium Zirconium Org. Synth.* **2002**, 355–389.